Accuracy of internal fields in volume integral equation simulations of light scattering

Hoekstra, A.; Rahola, J.; Sloot, P.

DOI
10.1364/AO.37.008482
Publication date
1998

Published in
Applied Optics

Scattering, New York, 99 (58)

2.3 INTERNAL FIELDS IN VOLUME INTEGRAL EQUATION SIMULATIONS OF LIGHT SCATTERING: ACCURACY AND RESONANCES

Alfons Hoekstra* (1), Jussi Rahola, (2) and Peter Sloot (1)
(1) University of Amsterdam, The Netherlands
(2) Center for Scientific Computing, Espoo, Finland

1. INTRODUCTION

In the Volume Integral Equation Formulation (VIEF) of simulations of elastic light scattering (see e.g. Lakhtakia and Mulholland, 1993) the internal field in a particle is first calculated. Next, the total and differential scattering cross sections are obtained from this internal field. Usually these cross sections are the required quantities, and their properties and the accuracy with which they are calculated have been studied extensively (Hage and Greenberg, 1990), also for the closely related Discrete Dipole Approximation (see e.g. Draine and Flatau, 1994). In some cases however the internal field itself is the required quantity.

We report on computer experiments to measure the accuracy of the internal fields as calculated by VIEF. The accuracy was obtained by considering spherical particles and comparing the simulated internal fields with those obtained by Mie theory.

Spheres can exhibit strong resonances in the internal field (see e.g. Videen et al., 1995). In this case one specific mode in the internal field is strongly amplified. We examine the case of such sharp internal field resonances.

2. METHODS

A sphere is discretised into N cubes. The internal field is obtained by VIEF on the center point of each cube. This field is denoted as $\mathbf{E}^i_{VIEF}$ where the index i refers to the field in the center of cube i. The exact Mie solution is also calculated in the centers of the cubes, and is denoted as $\mathbf{E}^i_{Mie}$. The difference field is defined as

$$\mathbf{E}^i_{diff} = \mathbf{E}^i_{Mie} - \mathbf{E}^i_{VIEF}. \quad (1)$$

In all simulations the sphere is centered at the origin and the incident field is an x-polarized plane wave traveling in the positive z-direction.

The model parameters are the size parameter x and the complex refractive index m of the sphere, and the size of cubes in the VIEF method, $d = \lambda/cpwl$, where *cpwl* stands for 'cubes per wavelength'.The size of the cubes is always specified in terms of the *cpwl* parameter. The accuracy of the internal fields are measured as a function of these 3 parameters.

The data sets are analysed in a number of different ways. The first method is by visualisation. The electric fields $\mathbf{E}^i_j$ (with j is *Mie*, *VIEF*, or *diff*) are three dimensional complex vector fields and are therefore difficult to visualise. A first approach is to calculate the energy density

$$s^i_j = \left(\mathbf{E}^i_j\right)^* \mathbf{E}^i_j , \quad (2)$$

where the * denotes complex conjugation. This scalar field is a measure of the intensity of the electric field, and can be plotted in color plots in a full 3D projection, or in planes through the sphere. This last method was applied by many other authors (e.g. Liu et al., 1995). Another way to visualise the data is to plot vector fields, which are obtained by either taking the real or imaginary parts of $\mathbf{E}^i_j$.

In this paper a number of examples of internal field visualisations will be shown in gray scale plots. We have prepared an accompanying document, available on the world wide web, where the color versions of the figures in this paper and a number of other examples of internal field visualisations are available (see http://www.wins.uva.nl/~alfons/int/int-f.html).

* *Corresponding author address: Alfons G. Hoekstra*, Univ. of Amsterdam, Dept. of Computer Science, Kruislaan 403, 1098 SJ Amsterdam, The Netherlands; e-mail: alfons@wins.uva.nl.

A final technique, that proved to be very useful, is to plot the amplitude of the electric fields as a function of the distance to the center of the sphere. Although all azimuthal information is no longer present, such plots give much information with respect to the distribution of e.g. the errors in the internal field.

Although visualisation is an indispensable tool in helping to understand the data sets, we also need quantitative error norms. The enormous amount of data (in this work N can be as large as 10^5) forces the use of statistical error norms. Define the absolute and relative error in the internal field on a point in the sphere as

$$\varepsilon^i_{abs} = \left|\mathbf{E}^i_{diff}\right| \text{ and } \varepsilon^i_{rel} = \left|\mathbf{E}^i_{diff}\right| \Big/ \left|\mathbf{E}^i_{Mie}\right|$$

Next, for both absolute and relative errors the minimum, maximum, mean, standard deviation, and root mean square errors (*RMS*) over all cube positions are calculated. This results in a good amount of data reduction. In most cases the *RMS*, combined with the maximum error, provides a good insight in the distribution of the errors.

3. RESULTS

We consider three typical case studies. The properties of the spheres are listed in Table 1. Fig. 1 shows the energy density of the internal field in the spheres in the x-z plane. Fig. 2 shows the energy density of the difference field.

number	size parameter	refractive index	cpwl	cpwl / Re(m)	N
1	9	1.05	15	14.3	41472
2	9	1.33 + 0.01 i	20	15.0	98512
3	5	2.5 + 1.4 i	35	14.0	90536

Table 1. Overview of size parameter and refractive index of the three spheres. The cpwl parameter is the "cubes per wavelength" as used in the VIEF simulation, and N is the number of cubes in the VIEF simulation.

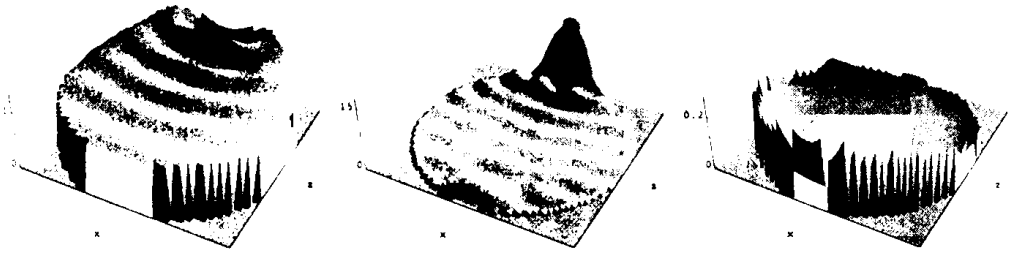

Figure 1. The energy density for the internal field obtained by Mie calculation. The left figure is for sphere 1, the middle figure for sphere 2, and the right figure for sphere 3. All scales in the plots are linear.

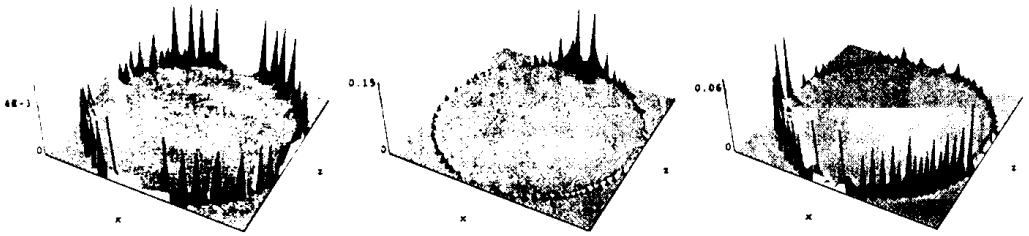

Figure 2: As in Fig. 1, but now for the energy density for the difference field, defined in Eq. 1.

One can observe three typical internal field distributions in Fig. 1. For a very small refractive index the internal field is almost equal to the incident field. For the larger refractive index of sphere 2 we

see a clear difference of the internal field and the incident field, and we observe a typical interference peak at the far end of the particle. Finally, for sphere 3, with a large absorption, we can see that the internal field is very small, except at the surface. Furthermore, the fields are strongest at the front end of the particle. These types of internal fields are in agreement with the cases surveyed by Dobson and Lewis (1989). As can be inferred from Figs. 1 and 2, in all three cases the errors in the VIEF internal fields are the largest on the surface of the sphere.

Another way to look at the internal field is to plot the amplitude of the internal field, and the amplitude of the difference field, as a function of the radial distance in the sphere. This is demonstrated in Fig. 3 for the difference field. The distribution of the errors in internal VIEF field is now clearly visible.

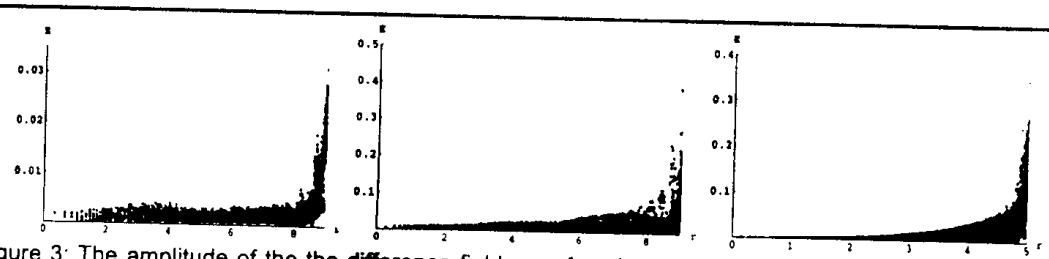

Figure 3: The amplitude of the the difference field as a function of radial distance in the sphere. The left column is sphere 1, the middle column sphere 2, and the right column sphere 3 (see Table 1 for properties of the spheres).

The relative RMS error of the internal fields for sphere 1 - 3 are 0.5, 2.8, and 23 % respectively. The maximum errors are 3.4, 19, and 120 % respectively.

Next, the convergence of VIEF simulations with respect to grid refinement is tested. For a number of different spheres the number of cubes per wavelength is gradually increased while keeping the size of the sphere fixed. A typical result is shown in Fig. 4.

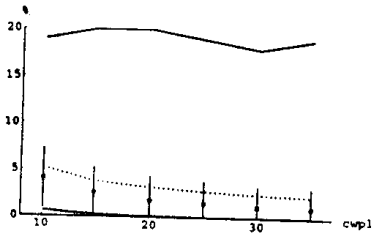

Figure 4. The relative errors in VIEF simulations of the internal field for a sphere with x = 5 and m = 1.33 + 0.01 i as a function of *cpwl*. The upper solid line is maximum error, the lower solid line the minimum error. The dots are the mean errors and the bars represent the standard deviation. The dashed line is the *RMS*.

The maximum error is more or less constant, and certainly does not decrease with increasing *cpwl*. These maximum errors in the internal field are always located on the surface of the sphere. All other statistical error norms (minimum, mean, standard deviation, and root mean square) show a monotonous decrease with increasing *cpwl*.

We finally investigate if VIEF simulations are able to reproduce resonances in Mie scattering. We identified two resonances which fall in the range of (x, m) values that can be covered by our VIEF simulations.

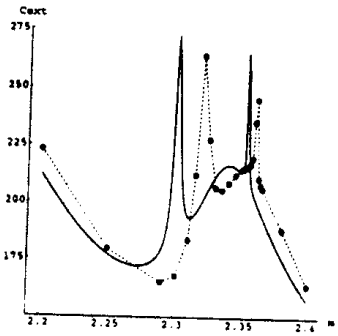

Figure 5. The extinction coefficient as a function of the refractive index for Mie calculations (the solid line) and VIEF simulations (the dots) for x = 4.875.

For a size parameter of x= 4.875 we found two values of m, close together, for which the Mie scattering becomes resonant, m = 2.3009279 and m = 2.3534695. They are a 7'th order TE (a_7) and an 8'th order TM (b_8) resonance respectively. Fig. 5 shows C_{ext} in the range $2.2 \leq m \leq 2.4$ for Mie calculations and for a number of VIEF simulations. In all VIEF simulations we take *cpwl* = 36.The Mie calculations

show the predicted resonances as two peaks on a smooth background. The VIEF simulations also show two sharp peaks, which are shifted to slightly larger values of m. This suggests that VIEF is able to reproduce the Mie resonances, but not at the exact positions.

The internal fields for the non-resonance case (e.g. for m = 2.2) resemble those of Fig. 1 for sphere 2. However, in case of the resonances, the internal field changes drastically. Here we only show results for the second resonance.

Fig. 6 shows the energy density for the second Mie resonance, i.e. m = 2.3534695. Notice the enormous difference in scales for the Mie resonance and the (non-resonant) VIEF simulation. The b_8 resonance is recognised by the fact that most energy density is located in the x = constant plane and 8 peaks in each half of the sphere.

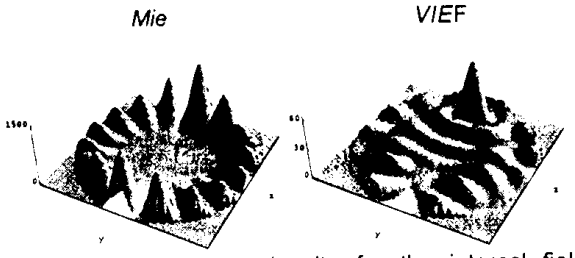

Figure 6. The energy density for the internal field obtained by Mie calculation (left) and VIEF simulation (right) for m = 2.3534695.

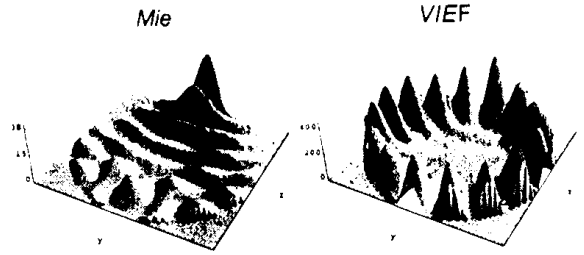

Figure 7. As in Fig. 5, but now for m = 2.36.

Fig. 7 shows the energy density for the second VIEF resonance, i.e. m = 2.36. In this case the b_8 resonance is clearly recognised in the VIEF results, although the amplitudes are smaller than those of the corresponding Mie resonance in Fig. 6. We have not carried out any more VIEF simulations in the immediate vicinity of m = 2.36. It is possible that for a slightly different refractive index the VIEF resonance is as strong as the Mie resonance.

4. DISCUSSION

The results of the extended sets of experiments on the accuracy of VIEF simulations of the internal field, of which part are presented in this paper, can be summarised as follows. The accuracy of the internal field simulations decreases with increasing refractive index. The largest errors always occur on the surface of the sphere, and the maximum errors seem to be independent of the size of the cubical cells. However, the average errors (mean, RMS) in the internal field decrease if the cubical cells are decreased in size. For a fixed value of the cubes per wavelength the errors in the internal field depend only very weakly on the size of the sphere. The VIEF simulations are capable of reproducing strong realistic resonances in the internal fields. However, the positions of the resonances on the refractive index axes (see Fig. 4) was slightly too large (0.9 % and 0.4 % for the first and second peak, respectively). The width and the height of the peaks in C_{ext} as a function of m for VIEF simulations are equal to those of Mie.

Currently we are preparing an extended manuscript describing in detail all experiments that were summarised in this paper.

5. REFERENCES

Draine, B.T. and Flatau, P.J., 1994: Discrete-dipole approximation for scattering calculations. *J. Opt. Soc. Am. A* **11**, 1491-1499.

Dobson, C.C. and I. Lewis, J.W., 1989: Survey of the Mie problem source function. *J. Opt. Soc. Am. A* **6**, 463-466.

Hage, J.I. and Greenberg, J.M., 1990: A model for the optical properties of porous grains. *Astrophys. J.* **361**, 251-259.

Lakhtakia, A. and Mulholland, G. W., 1993: On two numerical techniques for light scattering by dielectric agglomerated structures. *J. Res. Natl. Inst. Stand. Technol.* **98**, 699-716.

Liu, C., Kaiser, T., Lange, S., and Schweiger, G., 1995: Structural resonances in a dielectric sphere illuminated by an evanescent wave. *Optics Comm.* **117**, 521-531.

Videen, G., Li, J., and Chylek, P., 1995: Resonances and poles of weakly absorbing spheres. *J. Opt. Soc. Am. A* **12**, 916-921.